Supporting Information

Near-Zero Thermal Expansion Coordinated with Geometric Flexibility and π…π Interaction in Anisotropic $[Zn_8(SiO_4)(m\text{-}BDC)_6]_n$

Zhanning Liu,[a] Xingxing Jiang,[b] Chiming Wang,[c] Chenxi Liu,[c] Zheshuai Lin,[b] Jinxia Deng,[a] Jun Chen,[a] and Xianran Xing*[a]

a. Beijing Advanced Innovation Center for Materials Genome Engineering, Department of Physical Chemistry, University of Science and Technology Beijing, Beijing, 100083, China

b. Key Lab of Functional Crystals and Laser Technology, Technical Institute of Physics and Chemistry, Chinese Academy of Sciences, Beijing 100190, China

c. Beijing Key Laboratory for Science and Application of Function Molecular and Crystalline Materials, University of Science and Technology Beijing, Beijing, 100083, China

1. Synthesis

$[Zn_8(SiO_4)(m\text{-}BDC)_6]_n$ was synthesized by hydrothermal reaction. 1,3-benzenedicarboxylic acid ($m\text{-}H_2BDC$, 332 mg, 2 mmol) was dissolved in 2 mL NaOH (1M) solution, then 2 mL aqueous solution containing $Na_2SiO_3{\cdot}9H_2O$ (56.8 mg 2 mmol) was added. The pH of the solution was adjusted to 7 using 1M HNO_3 solution, and finally 1 mL aqueous solution containing $Zn(NO_3)_2\ {\cdot}6H_2O$ (594 mg 2 mmol) was added. After stirring under air for 10 minutes, the mixture was transfer to a 25 mL Teflon-lined reactor and the reactor was heated at 200°C for 100 hours, then gradually cooled to room temperature with a rate of 5°C/h. The colourless crystals were obtained and washed several times with deionized water.

2. Thermogravimetric analysis

Thermo-Gravimetric-Differential Scanning Calorimetry (TG-DSC) measurement was perfomed using a Labsys Evo system (by SETRAM) with a rate of $5°C{\cdot}min^{-1}$ under air.

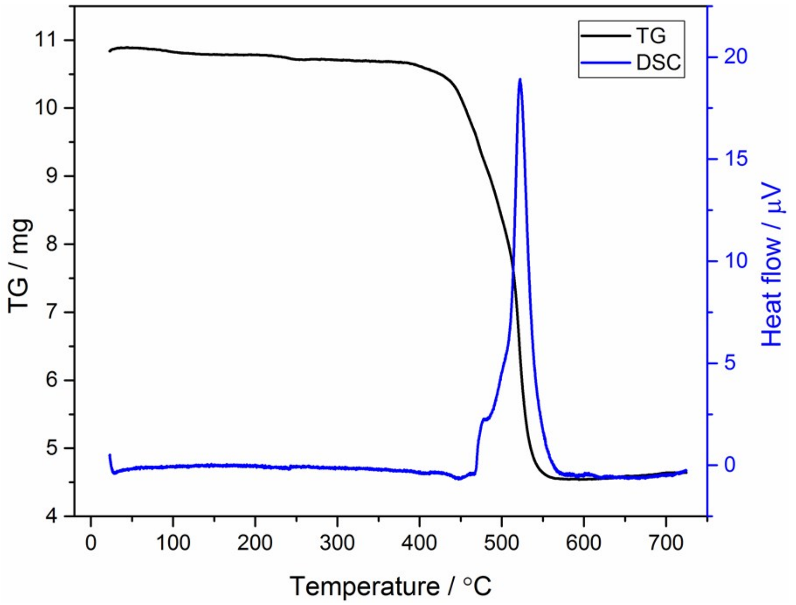

Figure S1 TG-DSC curves of $[Zn_8(SiO_4)(m\text{-}BDC)_6]_n$ measured under air.

3. Variable temperature high resolution syntchrotron X-ray powder diffraction

Variable temperature high resolution syntchrotron powder X-ray diffraction data was collected from 100 to 475 K with an interval of 25 K using the 11-BM-B beamline located at Advanced Photon Soures, Argonne National Laboratory. The sample was loaded into a 0.8mm diameter Kapton capillary. The capillary was spun at several radians per second to improve particle statistics.

Temperature was controlled from 100 to 475 K with a heating rate of 120 K/h using an Oxford Cryostream 700+ N_2 gas blower. Rietveld refinement to the diffraction data was used within GSAS[1] using the EXPGUI[2] interface (Figure S3). The exact wavelength (0.4127 Å) were determined from the reflections of a CeO_2 standard. The background was modelled by a shifted Chebyschev polynomial with 18 parameters. The scale factor, lattice parameters, zero point were also refined. The Pseudo-voigt function was choosen to generate the peak shapes. The coordinates and isotropic atomic displacement parameter were refined for all atoms except hydrogen atoms. The result of the final Rietveld refinement plot and results are shown in figure S3 and table S1. The lattice parameters extracted from Rietveld refinemetns are listed in Table S1.

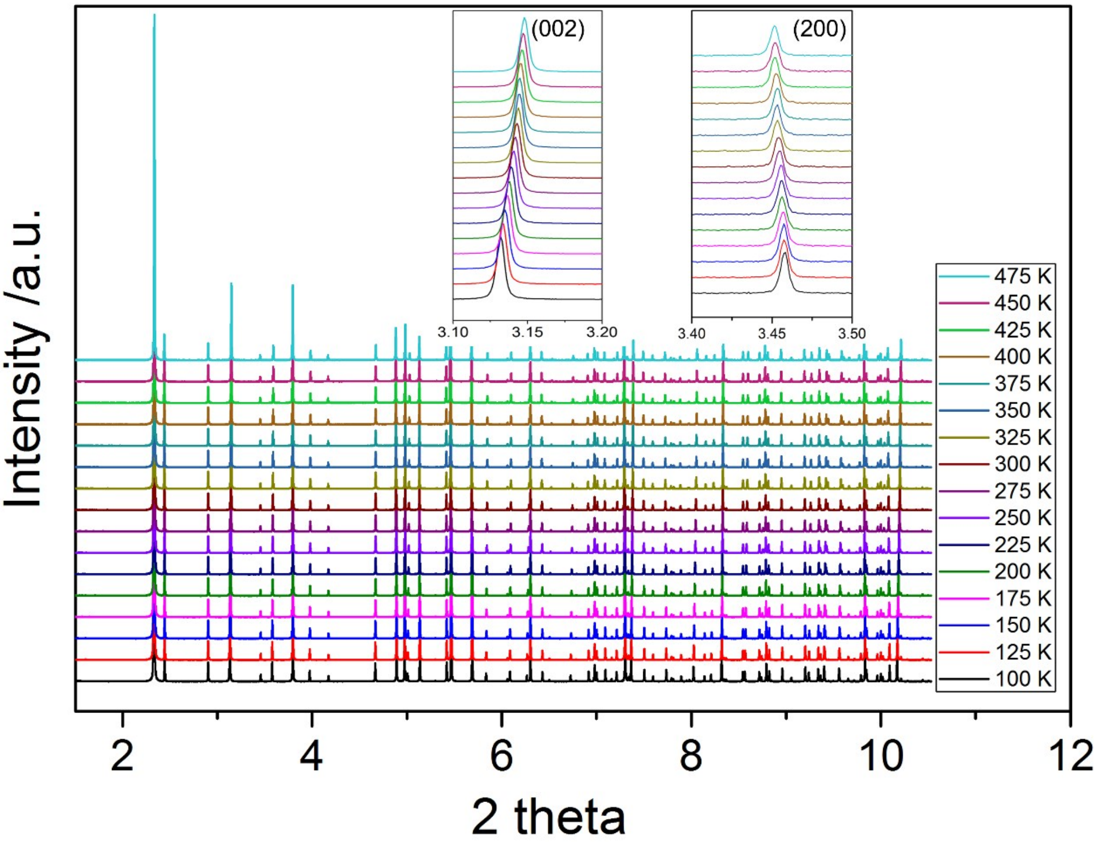

Figure S2 Temperature dependent synchrotron PXRD patterns of $[Zn_8(SiO_4)(m\text{-}BDC)_6]_n$. The two insets show the shift of reflections (002) and (200).

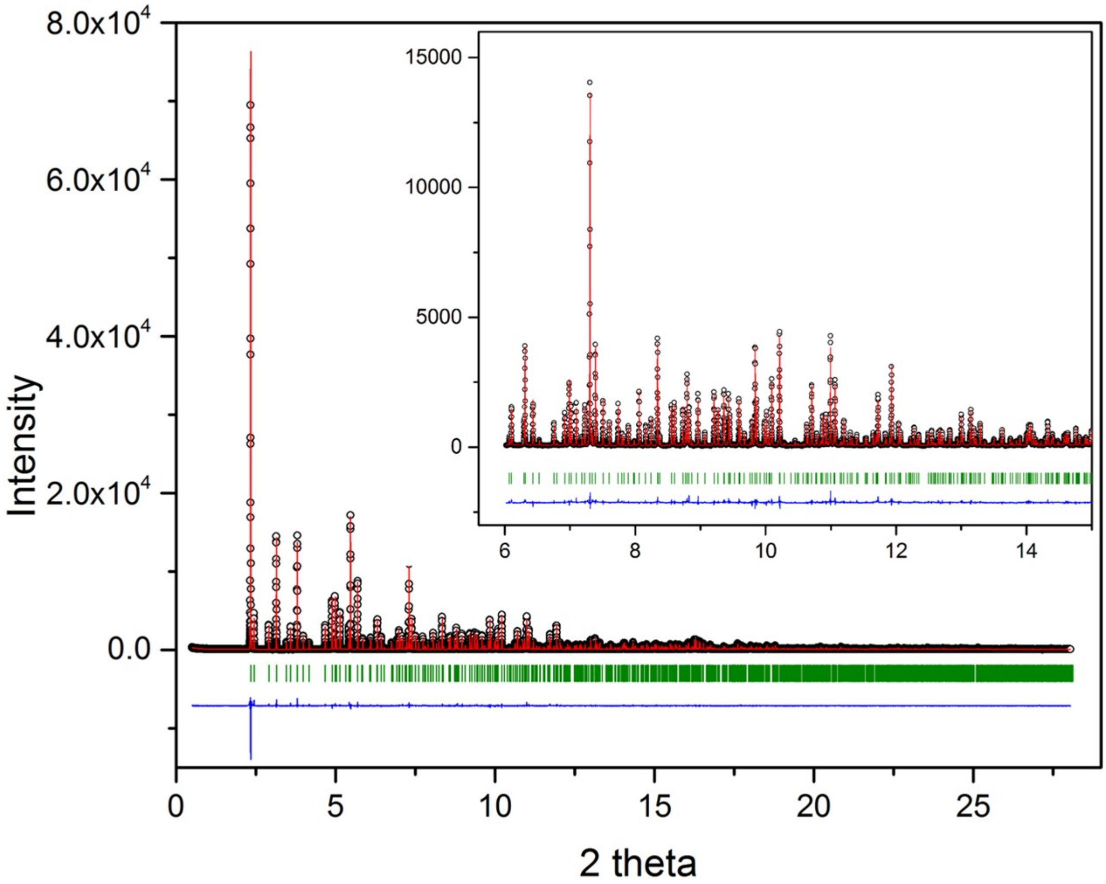

Figure S3 Final Rietveld refinement plot of [$Zn_8(SiO_4)$(*m*-BDC)$_6$]$_n$ at 300 K. A zoomed-in plot is shown in the inset. (R_p=6.99%, wR_p=9.45%, chi^2=2.322).

Table S1 Unit cell parameters obtained from Rietveld refinement to the synchrotron PXRD data

T / K	a / Å	c / Å	V / Å^3
100	13.66225(2)	15.08438(2)	2815.604(9)
125	13.66379(2)	15.07704(2)	2814.871(9)
150	13.66545(2)	15.07038(2)	2814.311(9)
175	13.66732(2)	15.06418(2)	2813.925(10)
200	13.66929(2)	15.05816(2)	2813.610(10)
225	13.67133(2)	15.05173(2)	2813.248(10)
250	13.67322(2)	15.04492(2)	2812.753(10)
275	13.67533(2)	15.03853(2)	2812.426(11)
300	13.67748(2)	15.03244(2)	2812.171(10)
325	13.67963(2)	15.02713(2)	2812.060(10)
350	13.68071(2)	15.02404(2)	2811.928(10)
375	13.68014(2)	15.02300(2)	2811.498(10)
400	13.68137(2)	15.01908(2)	2811.272(10)
425	13.68423(2)	15.01399(2)	2811.490(10)
450	13.68473(2)	15.01057(2)	2811.057(10)
475	13.68646(2)	15.00649(2)	2811.005(10)

4. Thermo-dilatometer measurement

Nearly 400 mg $[Zn_8(SiO_4)(m\text{-BDC})_6]_n$ was ground to powder using an agate mortar, and three drops of PVA agglomerant were added. Subsequently, the powder was pressed into a disk with a diameter of 10 mm and thickness of ~3 mm at 12 kN for 2 min. The formed disk was transferred to an oven at 280 ℃ for 2 h. The linear thermal expansion ($\Delta L/L$) of this disk was measured by the thermo-dilatometer (DIL 402 Expedis Select) with a rate of 5 K/min. The little difference of $\Delta L/L$ between the results of thermo-diatometer measurements and results extracted from the SXRD may be caused by the existence of PVA agglomerant.

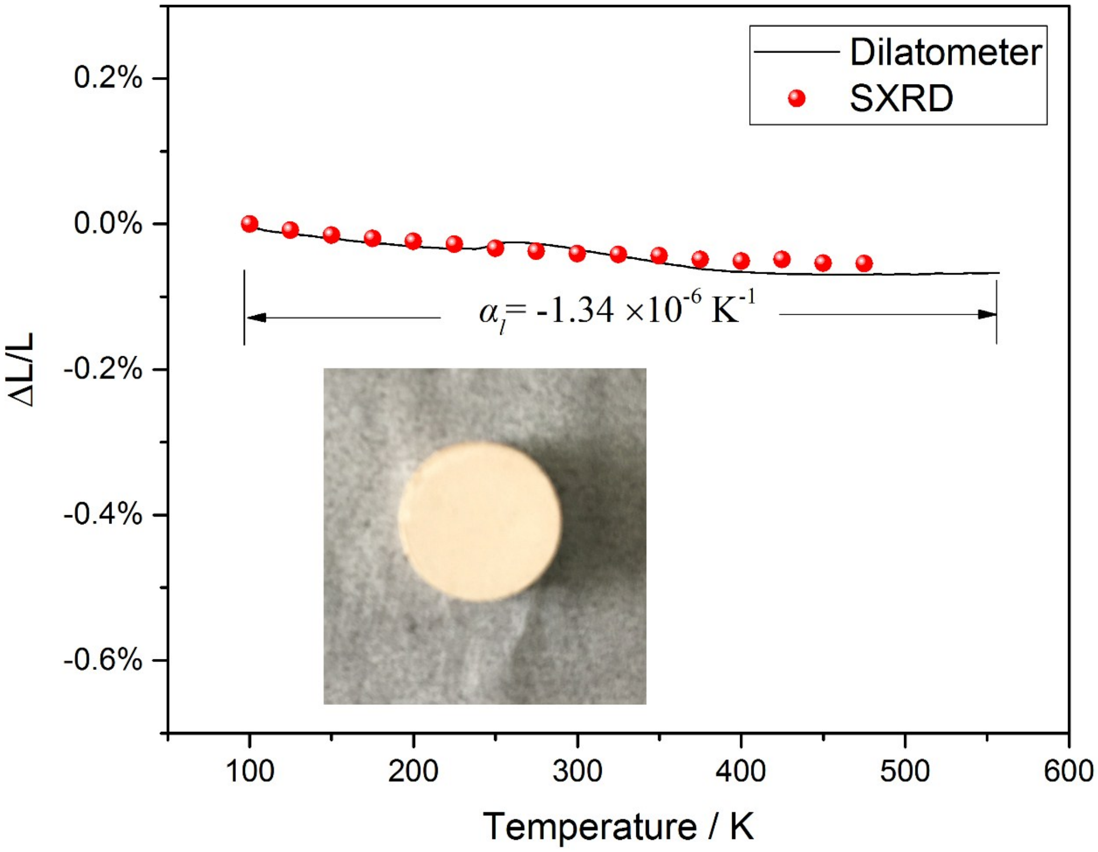

Figure S4. Linear thermal expansion behavior of $[Zn_8(SiO_4)(m\text{-BDC})_6]_n$ determined by a thermo-dilatometer (solid line) and isotopically averaged result from the Rietveld refinement. (Inset) Photograph of the pressed disk.

5. Variable temperature single crystal X-ray diffraction

Single crystal X-ray diffraction data were collected at the beamline BL26B1(Spring-8) using a wavelength of 0.7212 Å at 100 K, 150 K, 200 K, 250 K, and 300 K. The data were processed with HKL2000 programs. The structure was solved by the direct method (SHELX-2014)[3] through the OLEX2[4] and refined by full matrix least-squares on F^2. Anisotropic displacement parameters were used for the non-hydrogen atoms and isotropic parameters for the hydrogen atoms. Hydrogen atoms were added geometrically and refined using ridding model. CCDC 1827798-1827802 contain the supplementary crystallographic data for this paper.

Table S2 Crystal data of $[Zn_8(SiO_4)(m\text{-}BDC)_6]_n$ from variable temperature single crystal diffraction.

	100 K	150 K	200 K	250 K	300 K
Formula	$C_{48}H_{24}O_{28}SiZn_8$	$C_{48}H_{24}O_{28}SiZn_8$	$C_{48}H_{24}O_{28}SiZn_8$	$C_{48}H_{24}O_{28}SiZn_8$	$C_{48}H_{24}O_{28}SiZn_8$
Formula weight	1599.72	1599.72	1599.72	1599.72	1599.72
Temperature / K	100	150	200	250	300
Crystal system	tetragonal	tetragonal	tetragonal	tetragonal	tetragonal
Space group	$P4_2/n$	$P4_2/n$	$P4_2/n$	$P4_2/n$	$P4_2/n$
a / Å	13.6840(2)	13.6875(2)	13.6914(2)	13.6944(2)	13.6997(2)
b / Å	13.6840 (2)	13.6875(2)	13.6914(2)	13.6944(2)	13.6997(2)
c / Å	15.0654(3)	15.0535(3)	15.0409(4)	15.0329(4)	15.0187(3))
α / °	90	90	90	90	90
β / °	90	90	90	90	90
γ / °	90	90	09	90	90
Volume / Å^3	2821.01(10)	2820.25(11)	2819.47(12)	2819.22(11)	2818.73(9)
Z	2	2	2	2	2
ρ_{calc} g/cm^3	1.883	1.884	1.884	1.884	1.884
Reflections collected	4771	4937	4857	4813	4698
Independent reflections	2488	2494	2491	2499	2491
Data/restraints/parameters	2488/0/193	2494/0/193	2491/0/193	2499/0/193	2491/0/193
GOF on F^2	1.173	1.177	1.182	1.133	1.172
R_1,wR_2 [I>=2σ (I)]	R_1 = 0.0281, wR_2 = 0.0665	R_1 = 0.0278, wR_2 = 0.0699	R_1 = 0.0279, wR_2 = 0.0695	R_1 = 0.0272, wR_2 = 0.0670	R_1 = 0.0322, wR_2 = 0.0827
R_1,wR_2 [all data]	R_1 = 0.0305, wR_2 = 0.0676	R_1 = 0.0303, wR_2 = 0.0711	R_1 = 0.0305, wR_2 = 0.0709	R_1 = 0.0303, wR_2 = 0.0685	R_1 = 0.0343, wR_2 = 0.0840
CCDC number	1827798	1827801	1827799	1827800	1827802

6. Variable temperature Raman spectra study

The variable temperature Raman measurements were performed with a multichannel modular triple Raman system (JY-HR800) with confocal microscopy. The spot diameter of the focused laser beam on the sample is about 1 um. The solid-state diode laser (532nm) from Coherent Company-Verdi-2 was used as an excitated source. Sample temperature was controlled by a temperature-controlled stage (Linkam) between 100 and 600K.

The first-principles atomic vibration modes assignment was performed by the plane-wave pseudopotential density functional theory (DFT)[5-6] implemented by CASTEP package[7]. The generalized gradient approximation (GGA) with Perdew−Burke−Ernzerhof (PBE)[8] functional was adopted and the ion-electron interactions were modeled by the optimized normal-conserving pseudopotentials[9] for all elements. The kinetic energy cutoffs of 800 eV and Monkhorst-Pack[10] k-point meshes with the spanning grid less than 0.04/Å^3 in the Brillouin zone were chosen. Before the atomic vibration calculation, the crystal structure was fully optimized by Broyden–Fletcher–Goldfarb–Shanno (BFGS)[11] minimization scheme with the convergence criterions for energy, maximum force, maximum stress and maximum displacement set as 10^{-5} eV/atom, 0.03 eV, 0.05 GPa and 0.001 Å respectively. The vibrational property was calculated by linear response formalism[12], in which the phonon frequencies were obtained by the second derivative of the total energy with respect to the given perturbation[13]

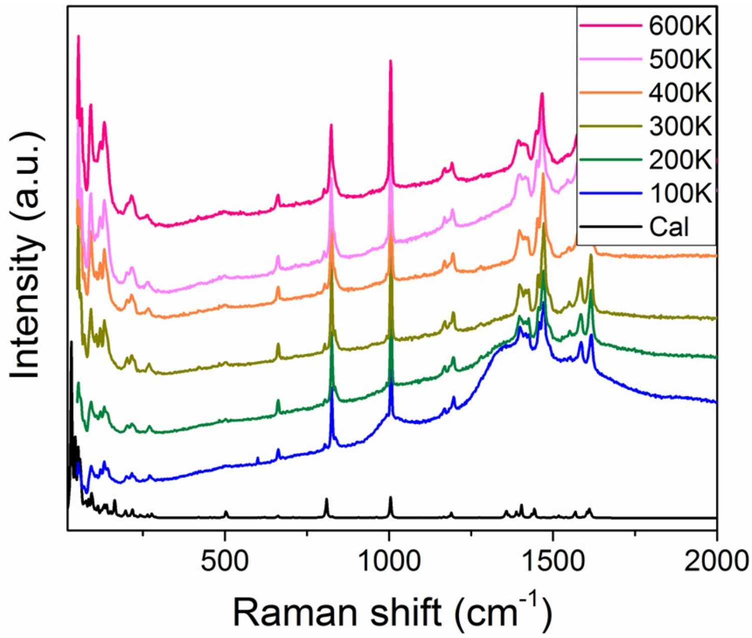

Figure S5 Temperature dependent Raman spectrum and the calculated result from DFT calculations (black).

7. Elastic properties calculated by DFT

The elastic constants were calculated by the finite-strain technology based on the geometrically optimized structure[13], in which the computational parameters were set as the same of the atomic vibration spectrum calculation. In elastic constants calculation, the maximum strain amplitude and the number of steps for each strain were set as 0.003 and 3 steps, respectively.

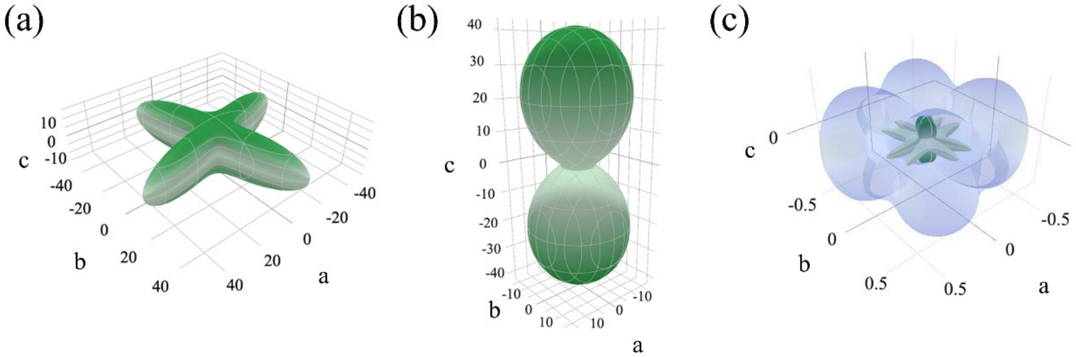

Figure S6 3D representations of anisotropic Young's modulus (in GPa, a), linear compressibility (b) and Poisson's ratios (c) for $[Zn_8(SiO_4)(m\text{-}BDC)_6]_n$. The Young's modulus in a given direction is shown as a green surface. Visualization generated using ELATE.[14]

8. Temperature dependent structural analysis

A topology simplification approach for this complex framwork was performed via the TOPOS program.[15] The cluster $Zn_8(SiO_4)$ cores and the *m*-BDC ligands were treated as the nodes of the underlying net. The distances of intemolecular $\pi ... \pi$ interactions are analysised via Platon program based on the Rietveld refinement results.[16]

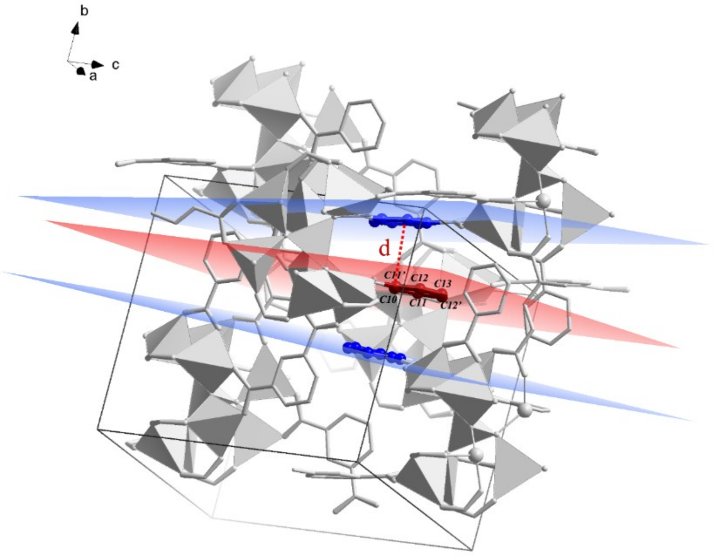

Figure S7 The schematic diagram of three $\pi ... \pi$ stacked phenyl rings. The three planes are not exactly parallel. The two blue planes are crystallographic equivalent.

Table S3 The distance of the central phenyl ring atoms to the upper plane in Figure S7.

Atom name	Distance to the upper plane (Å) at 100K	Distance to the upper plane (Å) at 475K
C10	3.4158	3.4674
C11	3.5598	3.7719
C11'	3.4133	3.4044
C12	3.5259	3.5678
C12'	3.7298	3.8335
C13	3.6905	3.7719

If we supposed that, the Si…Si unit is rigid (without $\pi ... \pi$ interaction), which means it won't change upon heating. With the same magnitude of geometric deformation (the same changes of β and the value of $d_{Si...Si}$ was fixed as 12.256), the lattice parameters can be calculated from the two equations below (Figure S8). The lattice parameters calculated from the geometric mathematical mode are listed in Table S4. It can be clearly seen that the geometric deformation will give rise to a positive volumetric thermal expansion.

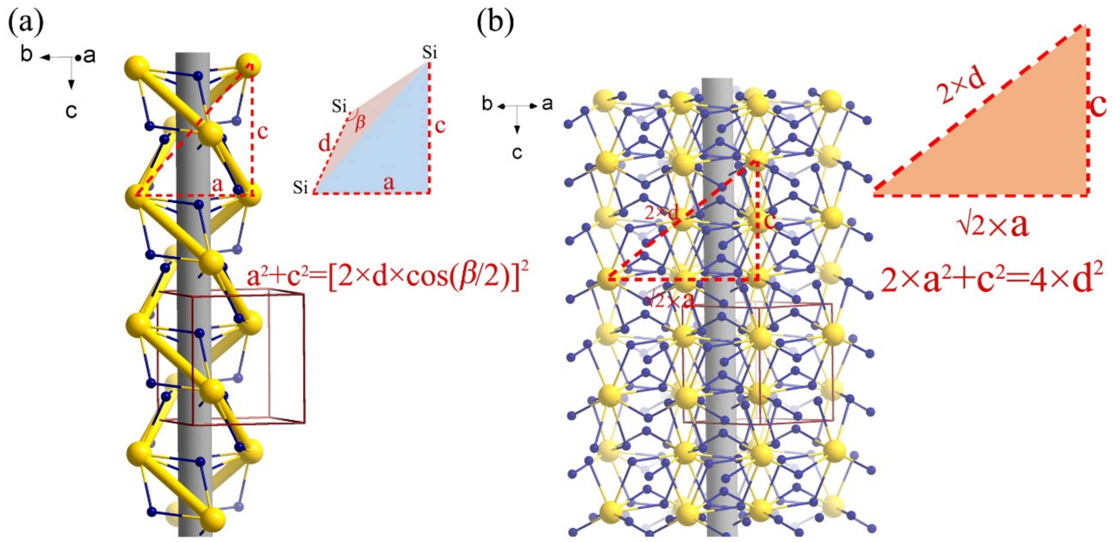

Figure S8 Geometric mathematical relations between the lattice parameter *a*, *c*, the building linkage length *d* and the angle *β* between connected $Zn_8(SiO_4)$ cores.

$$a^2 + c^2 = [2 \times d \times \cos(\frac{\beta}{2})]^2$$

$$2 \times a^2 + c^2 = 4 \times d^2$$

Table S4 Supposed that the Si…Si linkage is a rigid unit ($d_{Si…Si}$ won't change upon heating). The lattice parameter calculated from geometry mathematical model.

Temperature / K	β	$d_{Si…Si}$ / Å	a / Å	c / Å	V / Å^3
100	112.2527	12.256	13.6620	15.0843	2815.5010
125	112.2353	12.256	13.6652	15.0787	2815.7302
150	112.2189	12.256	13.6681	15.0733	2815.9473
175	112.2029	12.256	13.6708	15.0684	2816.1446
200	112.1871	12.256	13.6737	15.0631	2816.3567
225	112.1703	12.256	13.6766	15.0578	2816.5675
250	112.1532	12.256	13.6799	15.0518	2816.8033
275	112.1363	12.256	13.6828	15.0467	2817.0064
300	112.1200	12.256	13.6856	15.0414	2817.2109
325	112.1052	12.256	13.6883	15.0366	2817.3989
350	112.0969	12.256	13.6898	15.0339	2817.5014
375	112.0961	12.256	13.6899	15.0337	2817.5117
400	112.0859	12.256	13.6917	15.0304	2817.6394
425	112.0700	12.256	13.6945	15.0253	2817.8352
450	112.0620	12.256	13.6959	15.0227	2817.9339
475	112.0508	12.256	13.6981	15.0187	2818.0852

Table S5 Supposed that the angle *β* is a rigid unit (without geometric deformation). The lattice parameters calculated from geometry mathematical model.

Temperature / K	β	$d_{Si\ldots Si}$ / Å	a / Å	c / Å	V / Å
100	112.2527	12.256	13.66196	15.08418	2815.45095
125	112.2527	12.255	13.66085	15.08295	2814.76184
150	112.2527	12.254	13.65973	15.08172	2814.07285
175	112.2527	12.253	13.65862	15.08049	2813.38397
200	112.2527	12.252	13.6575	15.07926	2812.6952
225	112.2527	12.251	13.65639	15.07803	2812.00655
250	112.2527	12.25	13.65527	15.0768	2811.31801
275	112.2527	12.249	13.65416	15.07557	2810.62958
300	112.2527	12.249	13.65416	15.07557	2810.62958
325	112.2527	12.248	13.65304	15.07434	2809.94126
350	112.2527	12.248	13.65304	15.07434	2809.94126
375	112.2527	12.247	13.65193	15.07311	2809.25305
400	112.2527	12.247	13.65193	15.07311	2809.25305
425	112.2527	12.247	13.65193	15.07311	2809.25305
450	112.2527	12.246	13.65082	15.07187	2808.56496
475	112.2527	12.246	13.65082	15.07187	2808.56496

9. Reduced density gradient calculations

The reduced density gradient (RDG)[17] calculations were carried out to investigate the intramolecular force between benzene moietieson the basis of B3LYP[18-21]/6-311G(d)[22-24] using Gaussian 09 D.01 package[25] and Multiwfn 3.4[26], visualized by Visual Molecular Dynamics (VMD)[27].

Reference:

[1] A. C. Larson, R. B. Von Dreele, *Report lAUR* **1994**, 86-748.

[2] B. H. Toby, *Journal of applied crystallography* **2001**, *34*, 210-213.

[3] G. M. Sheldrick, *Acta Crystallographica Section C: Structural Chemistry* **2015**, *71*, 3-8.

[4] O. V. Dolomanov, L. J. Bourhis, R. J. Gildea, J. A. Howard, H. Puschmann, *Journal of Applied Crystallography* **2009**, *42*, 339-341.

[5] W. Kohn, L. J. Sham, *Physical Review* **1965**, *140*, 1133-&.

[6] M. C. Payne, M. P. Teter, D. C. Allan, T. A. Arias, J. D. Joannopoulos, *Reviews of Modern Physics* **1992**, *64*, 1045-1097.

[7] S. J. Clark, M. D. Segall, C. J. Pickard, P. J. Hasnip, M. J. Probert, K. Refson, M. C. Payne, *Zeitschrift Fur Kristallographie* **2005**, *220*, 567-570.

[8] J. P. Perdew, K. Burke, M. Ernzerhof, *Physical Review Letters* **1996**, *77*, 3865-3868.

[9] D. R. Hamann, M. Schluter, C. Chiang, *Physical Review Letters* **1979**, *43*, 1494-1497.

[10] H. J. Monkhorst, J. D. Pack, *Physical Review B* **1976**, *13*, 5188-5192.

[11] B. G. Pfrommer, M. Cote, S. G. Louie, M. L. Cohen, *Journal of Computational Physics* **1997**, *131*, 233-240.

[12] S. Baroni, S. de Gironcoli, A. Dal Corso, P. Giannozzi, *Reviews of Modern Physics* **2001**, *73*, 515-562.

[13] V. B. Deyirmenjian, V. Heine, M. C. Payne, V. Milman, R. M. LyndenBell, M. W. Finnis, *Physical Review B* **1995**, *52*, 15191-15207.

[14] R. Gaillac, P. Pullumbi, F.-X. Coudert, *Journal of Physics: Condensed Matter* **2016**, *28*, 275201.

[15] V. A. Blatov, *IUCr CompComm Newsletter* **2006**, *7*, 4-38.

[16] A. Spek, *Journal of Applied Crystallography* **2003**, *36*, 7-13.

[17] E. R. Johnson, S. Keinan, P. Mori-Sanchez, J. Contreras-Garcia, A. J. Cohen, W. Yang, *Journal of the American Chemical Society* **2010**, *132*, 6498-6506.

[18] A. Becke, *J. Chem. Phys.* **1993**, *98*, 5648.

[19] C. Lee, *Phys. Rev. B* **1988**, *37*, 785.

[20] S. Grimme, *The Journal of chemical physics* **2006**, *124*, 034108.

[21] S. Grimme, S. Ehrlich, L. Goerigk, *Journal of computational chemistry* **2011**, *32*, 1456-1465.

[22] R. Krishnan, *J. Chem. Phys.* **1980**, *72*, 650.

[23] A. McLean, *J. Chem. Phys.* **1980**, *72*, 5639.

[24] P. J. Hay, W. R. Wadt, *The Journal of Chemical Physics* **1985**, *82*, 299-310.

[25] M. Frisch, G. Trucks, H. Schlegel, G. Scuseria, M. Robb, J. Cheeseman, G. Scalmani, V. Barone, B. Mennucci, G. Petersson, *Gaussian Inc.: Wallingford, CT, USA* **2009**.

[26] T. Lu, F. Chen, *Journal of computational chemistry* **2012**, *33*, 580-592.

[27] W. Humphrey, A. Dalke, K. Schulten, *Journal of molecular graphics* **1996**, *14*, 33-38.